# High Accuracy Concentration Analysis of Accelerator Components in Acidic Cu Superfilling Bath

**Seunghoe Choe,[a] Myung Jun Kim,[a,*] Kwang Hwan Kim,[a] Hoe Chul Kim,[a] Yongkeun Jeon,[a] Tae Young Kim,[a] Soo-Kil Kim,[b,z] and Jae Jeong Kim[a,*,z]**

[a]*School of Chemical and Biological Engineering, Institute of Chemical Process, Seoul National University, Gwanak-gu, Seoul 151-744, Korea*
[b]*School of Integrative Engineering, Chung-Ang University, Dongjak-gu, Seoul 156-756, Korea*

We have devised a modified cyclic voltammetry stripping (CVS) method to measure the concentrations of bis-(sulfopropyl) disulfide (SPS) and 3-mercapto-1-propane sulfonate (MPS) in Cu plating solutions. Though MPS, a breakdown product of SPS, enhances the Cu deposition rate on flat electrodes, it is not a superfilling-capable accelerator for the damascene structure, unlike SPS. Therefore, accurate measurement of SPS in damascene Cu plating baths is important. However, enhancement of the Cu deposition rate by MPS interferes with the electrochemical signal of SPS, leading to a significant error when using the modified linear approximation technique (MLAT)-CVS analysis method. To evaluate their concentrations individually, a two-step CVS analysis was performed in which the total accelerator concentration ([SPS] + 1/2[MPS]) and conversion ratio were separately determined. All MPS species in the bath were oxidized to SPS by controlling the plating solution pH. Subsequent MLAT-CVS analysis successfully revealed the total accelerator concentration in the Cu plating solution. Individual SPS and MPS concentrations were thereby calculated using the conversion ratio evaluated from the difference in their relative accelerating abilities. This modified method enabled determination of the SPS concentration with <10% error, suggesting a reliable and high accuracy tool to predict pattern filling capabilities of plating solutions.
© The Author(s) 2015. Published by ECS. This is an open access article distributed under the terms of the Creative Commons Attribution Non-Commercial No Derivatives 4.0 License (CC BY-NC-ND, http://creativecommons.org/licenses/by-nc-nd/4.0/), which permits non-commercial reuse, distribution, and reproduction in any medium, provided the original work is not changed in any way and is properly cited. For permission for commercial reuse, please email: oa@electrochem.org. [DOI: 10.1149/2.0471602jes] All rights reserved.

Manuscript submitted September 8, 2015; revised manuscript received October 29, 2015. Published November 14, 2015.

Owing to the merits of high throughput, low process cost, and good film quality, Cu electroplating has a wide application, from traditional Cu foil production to state-of-the-art semiconductor metallization processes.[1–16] The Cu plating solution typically contains small amounts of organic additives,[1–16] which enhance the uniformity,[13] brightness,[14] and mechanical properties of the Cu film.[15] In addition, for particular application to damascene Cu plating, the additives enable bottom-up filling at trenches or vias by controlling the relative deposition rates of Cu at the top and bottom of the features.[1–12] For this application, the organic additives are grouped as the accelerator, suppressor, and leveler based on their electrochemical behaviors and their roles in pattern filling.

One of the most widely used accelerators is bis-(sulfopropyl) disulfide (SPS), a dimer of 3-mercapto-1-propane sulfonate (MPS). Acceleration by SPS in Cu superfilling has been explained by the competitive adsorption theory[17–21] or by the catalytic action caused by the reduction of cupric ions.[22,23] In the competitive adsorption theory, acceleration is regarded as a recovery of the deposition rate previously suppressed by the polyethylene glycol (PEG)-Cl inhibition layer, and recovery occurs through the displacement of the PEG-Cl layer with SPS.[17–19] A recent study revealed that the acceleration is a result of the dissociative adsorption of SPS with displacement of the well-ordered $Cl^-$ layer.[20,21] MPS, a dissociated product of SPS, reconverts to SPS with reduction of cupric ions, as described in Eq. 1.[20–23]

$$2MPS^- + 2Cu^{2+} \leftrightarrow SPS^{2-} + 2Cu^+ + 2H^+ \quad [1]$$

Here $Cu^+$ is further stabilized to form complex with residual MPS or $Cl^-$,[24] or rapidly oxidized by dissolved oxygen molecular.[25]

However, organic additives decompose through chemical/electrochemical side reactions during operation of the plating solution[26–35] or even under open circuit condition,[36,37] which leads to degradation of the plating solution. Decomposition of SPS during electroplating has been reported, as described in Eqs. 2 and 3.[26,31–34]

$$SPS^{2-} + O_2 + H_2O \rightarrow PDS^{2-} + MPS^- + H^+ \quad [2]$$

$$SPS^{2-} + 6H_2O \rightarrow 2PDS^{2-} + 10e^- + 12H^+ \quad [3]$$

Besides, Healy et al. has reported that SPS decomposes under open circuit condition by $Cu^+$, which comes from the comproportionation-disproportionation reaction between $Cu^{2+}$ and metallic Cu, to form Cu-thiolate complex.[36] They also have suggested that the Cu-thiolate complex is unstable in the presence of $O_2$ and undergoes oxidation.

By the reactions proposed in Eqs. 2 and 3, SPS continuously converts to MPS and 1,3-propane disulfonic acid (PDS). MPS is further regenerated to SPS though the reduction of cupric ions, as described in Eq. 1. As the processes of Eqs. 1–3 repeat, SPS gradually converts to PDS after a long period of operation of the plating solution.[26] Because of decomposition of the additives and the consequent degradation of the solution performance, concentration monitoring systems and additive feeding systems based on the measured concentrations are necessary to maintain the filling capability of the plating solution. A cyclic voltammetry stripping (CVS) method,[37–44] in combination with an experimental technique known as the modified linear approximation technique (MLAT),[41,44] has been widely used for this purpose. Using MLAT-CVS, the concentration of SPS is obtained by the following steps: 1) evaluation of $Q_i$ from CVS analysis of the suppressor-saturated plating solution (the intercept solution); 2) evaluation of $Q_0$ after addition of the target solution (Cu plating solution to be analyzed) into the intercept solution; 3) evaluation of Q after addition of the SPS standard solution into the intercept solution; 4) repetition of procedure 3 (2–3 times) to determine the increase in $\Delta Q/\Delta C_s$; and 5) evaluation of the SPS concentration in the target plating solution from the Eq. 4.

$$C = \frac{Q_0 - Q_i}{\Delta Q/\Delta C_s} \frac{V_t + V_i}{V_t} \quad [4]$$

Here $Q_i$, $Q_0$, and Q are the stripping charges of the intercept solution, the intercept solution mixed with the target solution, and the intercept solution after the addition of SPS standard solution, respectively. And, C is the concentration of SPS in target plating solution, $C_S$ is

*Electrochemical Society Active Member.
[z]E-mail: jjkimm@snu.ac.kr; sookilkim@cau.ac.kr

Downloaded on 2019-09-03 to IP 49.247.202.102 address. Redistribution subject to ECS terms of use (see ecsdl.org/site/terms_use) unless CC License in place (see abstract).

the concentration of SPS in intercept solution after addition of SPS standard solution, $V_i$ is the volume of intercept solution, and $V_t$ is the addition volume of target solution, respectively.

MLAT-CVS has been widely applied as a monitoring tool because it quickly determines the SPS concentration. However, conventional MLAT-CVS is unable to evaluate the by-product (MPS and PDS) concentrations in the Cu plating solution because this method is designed for a single accelerator system. Moreover, the electrochemically active byproducts, such as MPS, often lead to unreliable interference in the MLAT-CVS analysis.[44]

The influences of PDS and MPS have been discussed elsewhere. Our previous study and a recent study by Moffat et al. revealed that the effect of PDS is negligible because of the absence of active functional groups that affect the Cu deposition rate.[26,45] This indicates that PDS cannot interfere with the MLAT-CVS analysis of the SPS concentration. Contrary to the case of PDS, however, MPS has been known to enhance the Cu deposition rate despite its incapability of superfilling,[22] thus affecting the electrochemical behavior of the plating solution and filling capability.[22,23,44–47] Therefore, during conventional MLAT-CVS analysis, the presence of MPS gives rise to errors in the concentration of SPS, the real superfilling-capable accelerator.

In this work, we suggest a two-step CVS analysis for the individual measurement of SPS and MPS concentrations in acidic Cu plating solution. The suggested method is based on an assumption that the interconversion between SPS and MPS is strongly influenced by the solution pH because oxidation of MPS into SPS accompanies the formation of a proton (Eq. 1). In the first step, we determined the total accelerator concentration (conc. of SPS + 1/2 conc. of MPS) using the MLAT-CVS method, after oxidizing MPS into SPS by adjusting the Cu plating solution pH. Subsequently, in the second step we determined the conversion ratio from the result that acceleration by MPS was more effective than that by SPS. We finally obtained the concentrations of SPS and MPS separately using the values of the total accelerator concentration and conversion ratio.

## Experimental

Cu plating solutions, referred to as the target solution, intercept solution #1 (IS1), and intercept solution #2 (IS2), were used in this experiment. Target solutions comprised 0.25 M $CuSO_4$, 1.0 M $H_2SO_4$, 1 mM NaCl, 0–50 μM SPS, and 0–100 μM MPS. IS1 was a base solution for conventional MLAT-CVS analysis with a composition of 0.125 M $CuSO_4$, 0.5 M $H_2SO_4$, 1.0 mM NaCl, and 1400 μM PEG (MW: 3400). IS2 was a pH-modified IS1 consisting of 0.125 M $CuSO_4$, 0.5 M $H_2SO_4$, 1.0 mM NaCl, 1400 μM PEG (MW: 3400), and 1.2 M KOH. The composition of IS1 was optimized for conventional MLAT-CVS, while IS2 was optimized for the two-step CVS.

A pattern filling experiment was performed to verify the superfilling-capabilities of the target solutions having different compositions of SPS and MPS, and compare them with the two-step CVS results. The solution for pattern filling was composed of target solutions and 90 μM PEG (MW: 3400). Electroplating was carried out at room temperature with 10 mA/cm$^2$ current density. Cu pattern wafers with the structure of Cu seed (50 nm at the bottom of the trench, 15 nm at the sidewall)/Ta (30 nm at the bottom, 15 nm on the sidewall)/$SiO_2$ were used as the working electrodes. A Cu rod (99.9% purity) and Ag/AgCl [sat. KCl] were used as the counter and reference electrodes, respectively.

$^1$H-nuclear magnetic resonance (NMR) analysis was performed in order to observe the conversion of MPS into SPS under various pH conditions. Test samples were comprised of 1 mM $CuSO_4$, 500 μM MPS, and different amounts of $H_2SO_4$. The reference samples were comprised of 500 μM MPS or 250 μM SPS. The pH values of the test samples were adjusted to 0.3, 2, and 4 with $H_2SO_4$ prior to the addition of MPS. $D_2O$ was used as the solvent, and the analysis was performed after 20 min from the solution preparation.

CVS analysis was aimed at observing the electrochemical behavior of the solutions and measuring the concentrations of accelerators. CVS plots were obtained using either IS1 or IS2 as the base electrolyte. Prior to the CVS measurement, 0–4.5 μM SPS and 0–9 μM MPS were added into IS1 or IS2. A Pt rotating disk electrode with a rotating speed of 2000 rpm, a Pt rod, and Ag/AgCl (3 M KCl) were used as the working, counter, and reference electrodes, respectively. The reference electrode is sealed with outer plastic tube filled with 1 M $KNO_3$ to minimize $Cl^-$ leakage into the samples. A scan rate of 0.1 V/s and a vertex potential of -0.3 V were constantly applied.

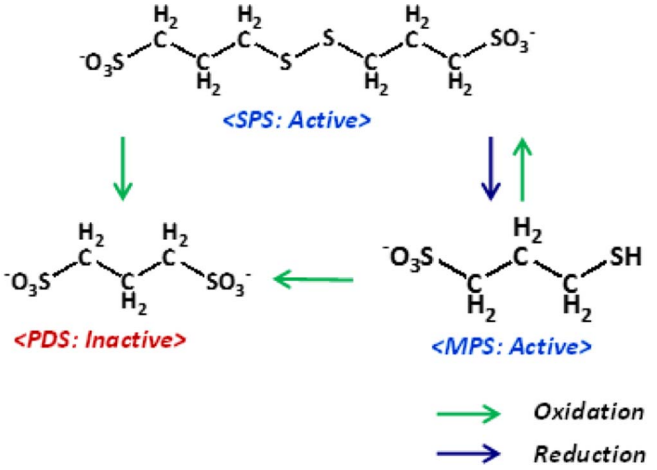


**Figure 1.** Redox reactions of SPS-related compounds during Cu electroplating.

Conventional MLAT-CVS analysis of the SPS concentration was carried out using the following procedures: 1) evaluation of $Q_i$ from the CVS analysis of IS1 (volume of IS1: 50 mL); 2) addition of diluter (1.0 mM NaCl) into the target plating solution at a 1:1 (v/v) ratio; 3) evaluation of $Q_0$ after addition of the diluted target solution into IS1 (addition volume: 5 mL); 4) evaluation of Q after addition of the standard SPS solution (5000 μM SPS) into IS1 (addition volume: 0.05 mL); 5) repetition of procedure 4 (3 times) to determine $\Delta Q/\Delta C_S$; and 6) evaluation of the SPS concentration of the target plating solution from Eq. 4.

However, our modified MLAT-CVS analysis consisted of a two-step methodology. The first step was carried out to evaluate the total accelerators concentration with the following procedures: 1) evaluation of $Q_i$ from the CVS analysis of IS2 (volume of IS2: 50 mL), 2) addition of pH adjuster (2.4 M KOH, 1.0 mM NaCl) into the target plating solution with a 1:1 (v/v) ratio, 3) evaluation of $Q_0$ after addition of the pH-adjusted target plating solution into IS2 (addition volume: 5 mL), 4) evaluation of Q after addition of the SPS standard solution (5000 μM SPS) into IS2 (addition volume: 0.05 mL), 5) repetition of procedure 4 (3 times) to determine $\Delta Q/\Delta C_S$, and 6) evaluation of the SPS concentration in the target plating solution from Eq. 4.

The second step was aimed at measuring the conversion ratio: 1) evaluation of $Q_i$ from the CVS analysis of IS1 (volume of IS1: 50 mL), 2) addition of diluter (1.0 mM NaCl) into the target plating solution with a 1:1 (v/v) ratio, 3) evaluation of Q after addition of the diluted target plating solution into IS1 (addition volume: 0.5–2 mL), 4) repetition of procedure 3 (3–5 times) to obtain the relation between $Q/Q_i$ and addition volume of the target plating solution, 5) evaluation of the slope for the calculation of $(\Delta Q/Q_i)/\Delta C_T$, where $C_T$ is the total accelerator concentration, and 6) evaluation of the conversion ratio using the pre-determined calibration curve. The conditions of all electrochemical experiments, including the electrodes, scan rate, and vertex potential, were as described above.

## Results and Discussion

Figure 1 shows the redox reactions of SPS-related compounds during Cu electroplating. As described by Eqs. 2 and 3, SPS continuously decomposes through chemical/electrochemical processes, forming MPS and PDS as its by-products.[26,31–34] PDS has been

Downloaded on 2019-09-03 to IP 49.247.202.102 address. Redistribution subject to ECS terms of use (see ecsdl.org/site/terms_use) unless CC License in place (see abstract).

known to have no effect on the electrochemical behavior and solution performance,[26,45] while the electrochemical influence of MPS is significant. Though MPS is known as a strong accelerator,[20–23] MPS itself is unable to induce superfilling[22] since superfilling is a result of complex behaviors of the accelerators, including not only the acceleration of the deposition kinetics but also its adsorption on the topographic surface and interaction with the suppressor. To acquire a superfilling capability, either SPS or aged MPS (dimerized into SPS) as described by Eq. 1[22] must be used. Based on those factors, the following two variables might be related to the superfilling capability of the plating solution.

$$1)\ \text{Concentration of total accelerating compounds } (C_T) = C_S + \frac{1}{2}C_M \quad [5]$$

$$2)\ \text{Conversion ratio of SPS to MPS } (X_S) = \frac{1/2C_M}{1/2C_M + C_S} = \frac{C_M}{2C_T} \quad [6]$$

where $C_S$ and $C_M$ are the concentrations of SPS and MPS, respectively. Physically, $C_T$ refers to the sum of intact and dissociated SPS (note that the dissociation of 1 molecule of SPS forms 2 molecules of MPS), while $X_S$ indicates the mole fraction of dissociated SPS. Namely, the decrease of $C_T$ implies the consumption of SPS by incorporation and oxidative decomposition resulting in PDS formation,[26] while the increase of $X_S$ means the consumption of SPS by dissociation to form MPS.

Figure 2 shows the CVS voltammogram as a function of artificially controlled $X_S$ at the same $C_T$ of 4.5 μM. It was observed that the stripping current density in a potential range of 0.05 V–0.35 V increased as $X_S$ increased. This means that 2 equivalents of MPS was more effective than 1 equivalent of SPS in accelerating Cu reduction on the flat electrode, as reported by Tan et al. and Moffat et al. who observed the stronger acceleration effect of MPS than SPS using chronoamperometry experiments.[46,47]

Despite the superfilling-incapability of MPS, its electrochemical acceleration effect, as shown in Figure 2 and the literature,[22,23,44–46] might lead to significant error in the results of conventional MLAT-CVS analysis since the electrochemical responses of SPS and MPS are not distinguishable in the conventional MLAT-CVS. (Note that conventional MLAT-CVS provides only a stripping charge value, regardless of where the increased stripping charges originate—from either MPS or SPS). Table I shows the measured C values by conventional MLAT-CVS analysis of various plating solutions having different $C_S$ and $C_M$. This confirms that the accuracy of conventional MLAT-CVS is guaranteed only when $X_S = 0$ ($C_M = 0$). Otherwise, the C value is always higher than the actual $C_S$ because of the acceleration effect by MPS. Furthermore, the measured C values exhibit

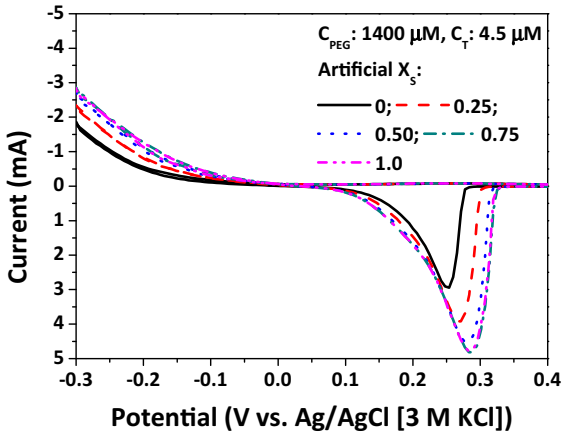


**Figure 2.** CVS results showing the influence of $X_S$ on the accelerating effect. The electrolyte was composed of 0.125 M $CuSO_4$, 0.5 M $H_2SO_4$, 1.0 mM NaCl, 1400 μM PEG (MW: 3400) and different amounts of MPS and SPS. The concentration of total accelerating compounds ($C_T$) was maintained as 4.5 μM and the conversion ratios of SPS to MPS ($X_S$) were given by controlling the amounts of MPS and SPS.

**Table I. Measured concentrations of accelerator with conventional MLAT-CVS analysis.**

| | Actual values | | | | Conventional CVS |
|---|---|---|---|---|---|
| Solution | $C_S$ (μM) | $C_M$ (μM) | $C_T$ (μM) | $X_S$ | C* (μM) |
| #1 | 50 | 0 | 50 | 0 | 50.32 (±1.97) |
| #2 | 40 | 20 | 50 | 0.2 | 55.07 (±2.31) |
| #3 | 30 | 40 | 50 | 0.4 | 86.96 (±5.64) |
| #4 | 25 | 0 | 25 | 0 | 24.46 (±1.29) |
| #5 | 20 | 10 | 25 | 0.2 | 24.32 (±1.64) |
| #6 | 15 | 20 | 25 | 0.4 | 36.16 (±2.04) |

*Note that C is conventionally treated as $C_S$.

significant deviation from $C_T$ due to the strong accelerating ability of MPS compared to that of SPS.

Figure 3 presents the filling performances of plating solutions #1–#6 (refer to Table I for details). As shown in Figures 3a–3f, the filling capability is a strong function of $X_S$ (i.e. $C_S$ and $C_M$); the increase of $X_S$ leads to degradation of the filling capability. The bumps are clearly observed only when $X_S = 0$ (or $C_M = 0$) as shown in Figures 3a and 3d. Otherwise, the filling profile seems to change into either conformal

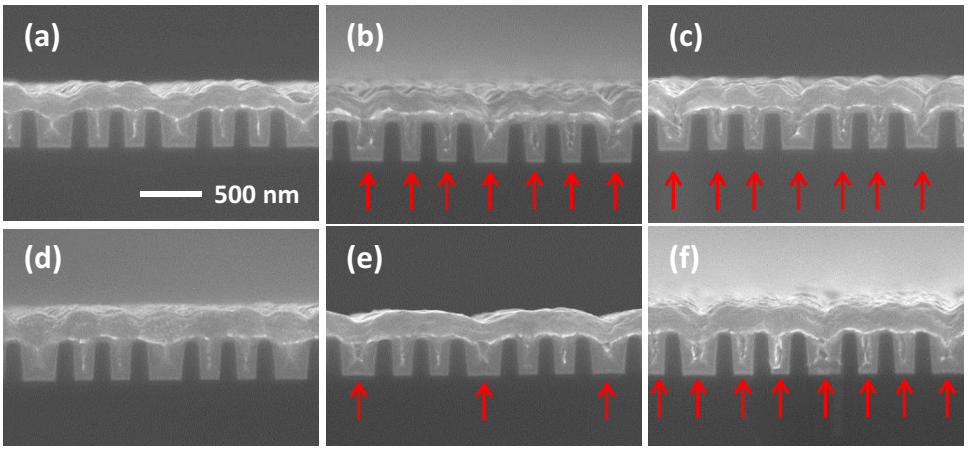


**Figure 3.** Filling performances of plating solutions (a) #1, (b) #2, (c) #3, (d) #4, (e) #5, and (f) #6 (see Table I for details).

Downloaded on 2019-09-03 to IP 49.247.202.102 address. Redistribution subject to ECS terms of use (see ecsdl.org/site/terms_use) unless CC License in place (see abstract).

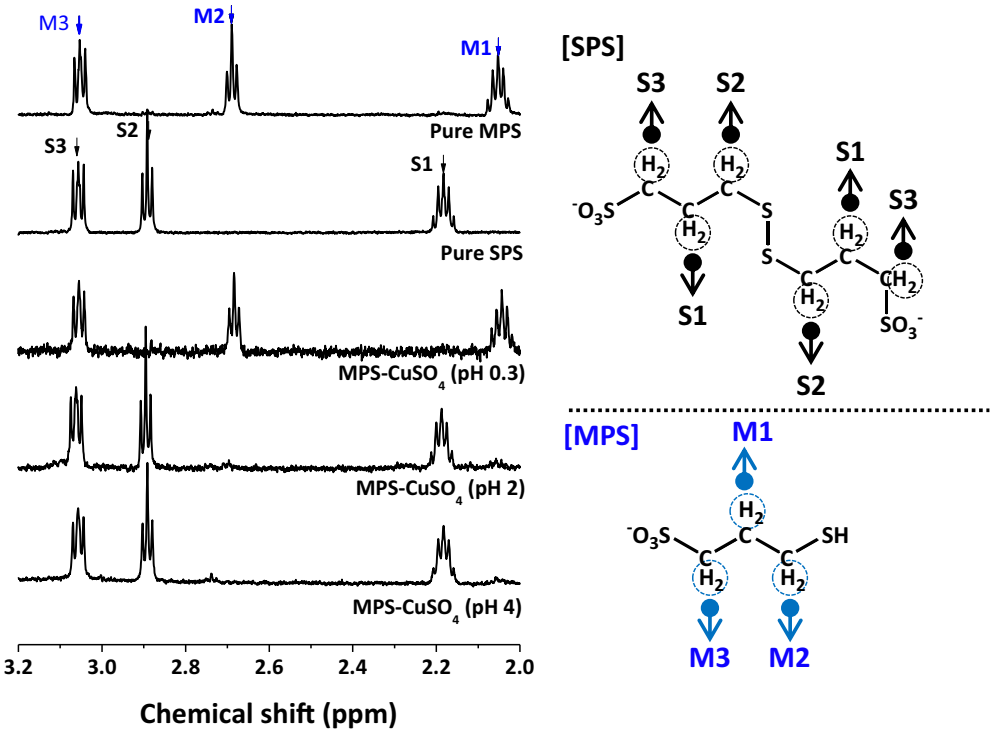


**Figure 4.** $^1$H-NMR results of MPS in $D_2O$ solutions containing 1 mM $CuSO_4$ and different amounts of $H_2SO_4$ as a pH adjuster. For the comparison, $^1$H-NMR results of SPS and MPS in pure $D_2O$ were also presented.

or sub-conformal generating voids or seams (indicated by arrows) as $X_S$ increases. Similar results were reported by Kim et al. showing that MPS itself is unable to induce bottom-up filling, whereas its dimerized form, SPS, enabled superfilling.[22] One notable point is the adverse effect of MPS on the filling capability. Figures 3a and 3d show that in the absence of MPS in the plating solution, an SPS concentration within the range of 25–50 μM is sufficient to induce superfilling. However, as shown in Figures 3b and 3c, the use of solutions #2 and #3, containing 20–40 μM MPS, result in a conformal filling profile, which implies that the presence of MPS causes deterioration of the filling capability.

Figure 3 shows that $C_M$ and $C_S$ are critical factors in determining the filling performance of the plating solution. However, as revealed in Table I, conventional MLAT-CVS is unable to determine the $C_S$ and $C_M$ separately. A new method is necessary in which the two variables ($C_T$ and $X_S$) can be separately measured, and $C_T$ can be obtained by sequential steps of artificial conversion of MPS to SPS (i.e. establishing the condition of $X_S = 0$) and then measuring the C value using MLAT-CVS (note that $C = C_S = C_T$ when $X_S = 0$). In detail, the first step aims to evaluate $C_T$ by the intentional control of another variable ($X_S$) with pH adjustment of the target plating solution. Figure 4 presents the $^1$H-NMR spectra of MPS in the Cu plating solutions with pH = 0.3, 2, and 4 after 20 min in the open circuit condition. The molecular structures with labeled hydrogens were taken from the authors previous work.[26] For the case of pH = 0.3, the chemical structure of MPS remains, whereas for weak acidic conditions of pH = 2 and 4, MPS completely converts to SPS within 20 min. This is because the forward reaction of Eq. 1 is promoted in relatively high pH conditions by Le Chatelier's principle. Fast thiol oxidation to disulfide at high pH has been reported elsewhere, including protein engineering.[48] Similar NMR study by Garcia-Cardona et al. demonstrated the formation of SPS and Cu-thiolate complex from the reaction between MPS and $Cu^{2+}$ in moderate pH condition (0.25 M $D_2SO_4$).[24] This work also supports that SPS is originated from reaction 1, though the different pH with our work might cause the different conversion rate.

Figure 5 presents the CVS results with various $X_S$ values for the case of pH = 2. The current densities and corresponding stripping charges are independent of $X_S$, unlike in strong acidic conditions of pH = 0.3 (Figure 2). As shown in the $^1$H-NMR results (Figure 4), this seems to result from complete oxidation of MPS into SPS.

The pH adjustment of the target plating solutions led to the condition of $X_S = 0$ ($C_M = 0$), resulting in identical CVS plots, regardless of the initial $X_S$ values. As shown in Table I, C values from conventional MLAT-CVS match well with $C_T$ in the case of $X_S = 0$. This means that $C_T$ can now be evaluated with MLAT-CVS analysis after

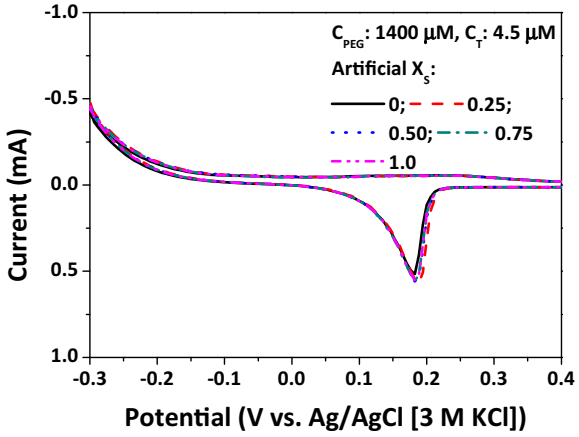


**Figure 5.** CVS results with various $X_S$ values after pH adjustment. The electrolyte was composed of 0.125 M $CuSO_4$, 0.5 M $H_2SO_4$, 1.0 mM NaCl, 1400 μM PEG (MW: 3400), 1.2 M KOH (pH adjuster) and different amounts of MPS and SPS. The concentration of total accelerating compounds ($C_T$) was maintained as 4.5 μM and the conversion ratios of SPS to MPS ($X_S$) were given by controlling the amounts of MPS and SPS. The pH of the electrolyte was maintained as 2 by adding KOH solution to the electrolyte.

Downloaded on 2019-09-03 to IP 49.247.202.102 address. Redistribution subject to ECS terms of use (see ecsdl.org/site/terms_use) unless CC License in place (see abstract).

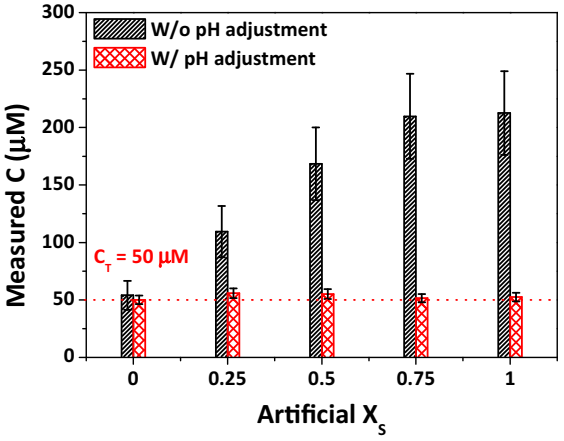


**Figure 6.** MLAT-CVS results of accelerator concentrations in Cu plating solutions with and without pH adjustment.

pH adjustment of the plating solution. Figure 6 shows the measured concentrations by MLAT-CVS for 50 μM $C_T$ with various $X_S$ values before and after pH adjustment. It was observed that in the case without pH adjustment, the measured $C_T$ value increases as $X_S$ increases due to the stronger accelerating ability of MPS than SPS. However, when the pH of the target solution is adjusted, the measured $C_T$ values are in good agreement with the actual $C_T$ values of 50 μM, regardless of the initial $X_S$.

The above results show that $C_T$ can be accurately measured by MLAT-CVS analysis after pH adjustment. However, $C_T$ itself cannot fully indicate the filling capability of the plating solution because the filling capability strongly depends on not only $C_T$ but also $X_S$ (Figure 3). Therefore, additional analysis to measure $X_S$ must be developed, which can be performed based on the result that the acceleration effect of MPS is relatively stronger than that of SPS (Figure 2). This means that $X_S$ influences the current density and stripping charges in the CVS analysis, as presented in Figure 7. Figure 7a shows that the stripping charge increases linearly with the increase in $C_T$, and the slopes of the plot, $(\Delta Q/Q_i)/\Delta C_T$, are affected by $X_S$. Figure 7b presents the relation between $(\Delta Q/Q_i)/\Delta C_T$ and $X_S$, which reveals that $(\Delta Q/Q_i)/\Delta C_T$ linearly increases as $X_S$ increases in the range of $X_S < 0.5$. This relationship will be further used in the independent determination of $C_M$ and $C_S$.

Figure 8 presents the procedures of the two-step CVS for determination of $C_T$ and $X_S$. In the first step, the pH adjustment of the target plating solution was carried out in order to oxidize MPS into SPS, using an alkaline solution consisting of 2.4 M KOH and 1.0 mM NaCl. Then, MLAT-CVS analysis was performed to determine $C_T$. In the second step, the target solution was diluted with 1.0 mM NaCl in a 1:1 ratio, which was added to IS1 3–5 times. The stripping charges were measured after each addition, from which the graph for $Q/Q_i$ vs. addition volume of the target solution was obtained. The addition volume of the target plating solution can be converted to $C_T$ of IS1 using the following equation.

$$C_{TI} = \frac{C_{Tt} \cdot V_t}{V_{IS1} + V_t} \quad [7]$$

where $C_{TI}$ is the $C_T$ value of IS1 after addition of the target plating solution, $C_{Tt}$ is the $C_T$ of the target plating solution, $V_t$ is the addition volume of the target plating solution, and $V_{IS1}$ is the initial volume of IS1. Therefore, the plot of $Q/Q_i$ vs. $C_{TI}$ could be obtained, in which $(\Delta Q/Q_i)/\Delta C_{TI}$ is converted to $X_S$ using the calibration curves presented in Figure 7b. The values of $C_{Tt}$ and $X_S$ were then used to determine $C_S$ and $C_M$, as described in Eqs. 8 and 9.

$$C_M = 2C_{Tt}X_S \quad [8]$$

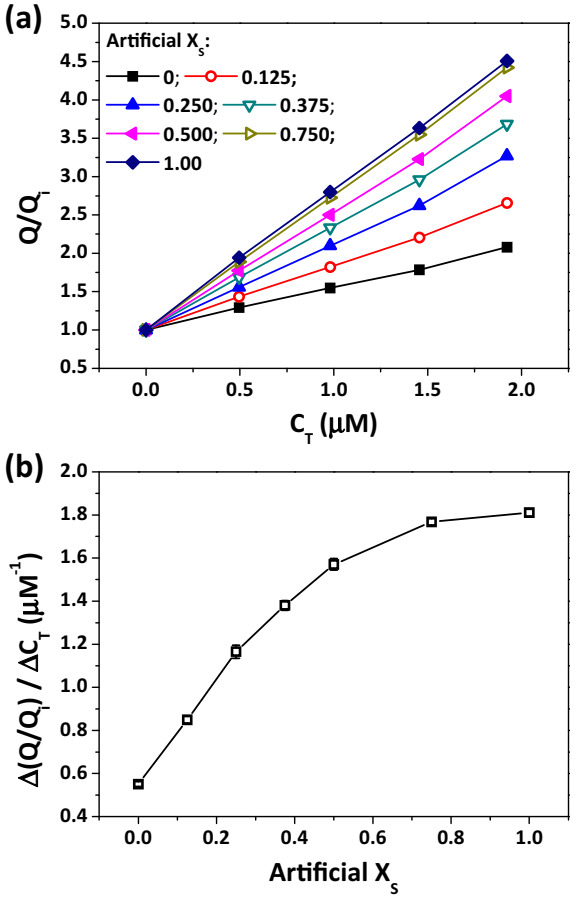


**Figure 7.** (a) $Q/Q_i$ as a function of $C_T$ with various $X_S$ values. The slope of the $Q/Q_i$ vs. $C_T$ plot is presented in (b).

$$C_S = C_{Tt}(1 - X_S) \quad [9]$$

The accuracy of the two-step MLAT-CVS analysis was verified using the same test samples of solutions #1–#6 (Table I) and the results are presented in Table II. Table II shows now the complete sets of $C_S$, $C_M$, $C_T$, and $X_S$ values for solutions #1–#6. The C values from conventional MLAT-CVS and filling performances of solutions #1–#6 are also presented for comparison. As shown in Table I, the conventional MLAT-CVS provides only the concentration (C), which is not in good agreement with the actual $C_S$ except when $X_S = 0$ ($C_M = 0$). In addition, the conventional MLAT-CVS cannot provide $C_M$, which limits the accurate assessment of solution performance. However, for the case of the modified two-step MLAT-CVS, both $C_M$ and $C_S$ were accurately measured within 10% error. By providing $X_S$ values, the superfilling-capability of the test solutions is now also predictable without actual filling tests; an extremely low $X_S$ (close to zero) corresponds to good superfilling performance. These results indicate the powerful ability of the developed two-step MLAT-CVS as a monitoring tool for Cu superfilling baths.

## Conclusions

A modified two-step MLAT-CVS method was suggested as a powerful tool for evaluation of $C_S$ (concentration of SPS) and $C_M$ (concentration of MPS) in an acidic Cu plating bath. This method is designed to determine two important parameters (the total accelerator concentration $C_T$ and the conversion ratio $X_S$) governing the filling capability of the plating solution. In order to obtain $C_T$, the condition of $X_S = 0$ was established by intentional pH control of the target plating solution,

Downloaded on 2019-09-03 to IP 49.247.202.102 address. Redistribution subject to ECS terms of use (see ecsdl.org/site/terms_use) unless CC License in place (see abstract).

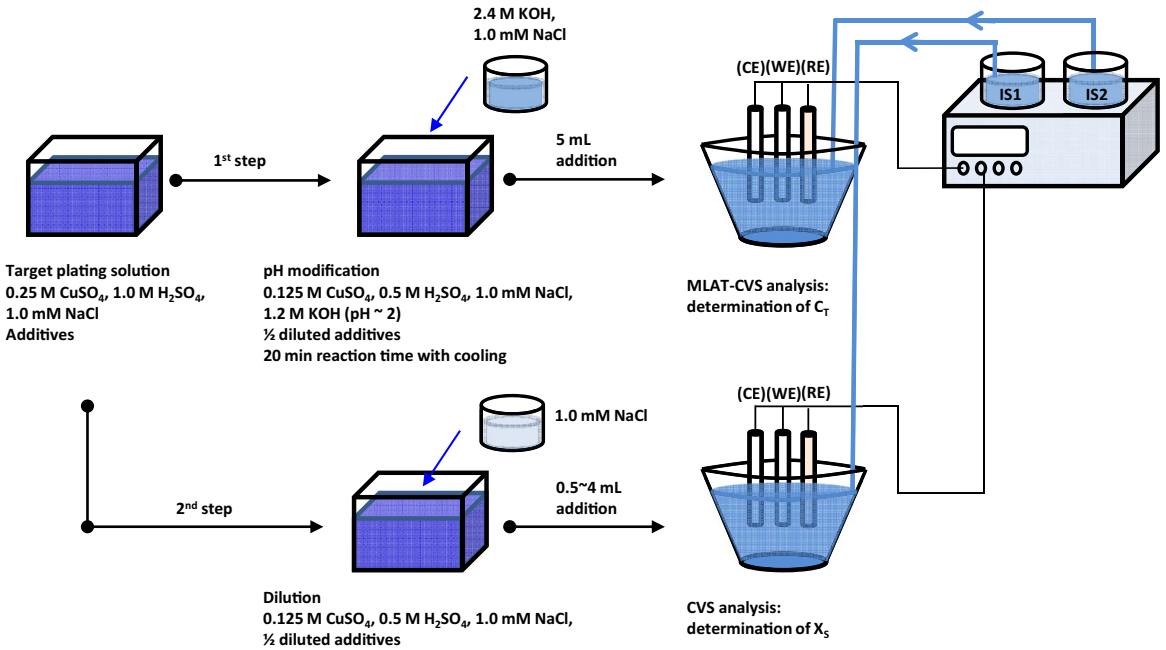


**Figure 8.** Modified CVS analysis procedure.

**Table II. Measured $C_T$, $X_S$, $C_S$, and $C_M$ with modified CVS analysis. The C values from conventional MLAT-CVS analysis are also presented as reference.**

| | Actual values | | | | Conventional CVS | Modified CVS | | | | |
|---|---|---|---|---|---|---|---|---|---|---|
| Solution | $C_T$ (μM) | $C_S$ (μM) | $C_M$ (μM) | $X_S$ | C* (μM) | $C_T$ (μM) | $C_S$ (μM) | $C_M$ (μM) | $X_S$ | Filling performance |
| #1 | 50 | 50 | 0 | 0 | 50.32 (±1.97) | 50.07 (±2.06) | 49.77 (±2.08) | 0.60 (±0.02) | 0.006 | Good |
| #2 | 50 | 40 | 20 | 0.2 | 55.07 (±2.31) | 51.76 (±2.76) | 42.24 (±2.57) | 19.05 (±1.01) | 0.184 | Bad |
| #3 | 50 | 30 | 40 | 0.4 | 86.96 (±5.64) | 50.09 (±2.48) | 32.05 (±2.11) | 36.06 (±1.78) | 0.360 | Bad |
| #4 | 25 | 25 | 0 | 0 | 24.46 (±1.29) | 24.28 (±1.49) | 23.43 (±1.46) | 1.70 (±0.10) | 0.035 | Good |
| #5 | 25 | 20 | 10 | 0.2 | 24.32 (±1.64) | 25.30 (±2.10) | 20.50 (±1.91) | 9.61 (±0.80) | 0.190 | Bad |
| #6 | 25 | 15 | 20 | 0.4 | 36.16 (±2.04) | 26.38 (±2.65) | 16.77 (±2.29) | 19.20 (±1.93) | 0.364 | Bad |

*Note that C is conventionally treated as $C_S$.

whereby MLAT-CVS analysis could reveal $C_T$ without the interference of MPS. $C_T$ was then converted to individual concentrations, $C_S$ and $C_M$, using $X_S$ evaluated from the difference of the relative accelerating abilities between SPS and MPS. This modified method quickly provided $C_S$ and $C_M$ of the sample baths with less than 10% error, enabling the accurate prediction of the filling performance of the solution without actual filling tests.

## Acknowledgment

This work was supported by the Technology Innovation Program (10043789) funded by the Ministry of Knowledge Economy (MKE, Korea). This research was also supported by the Basic Science Research Program through the National Research Foundation of Korea (NRF) funded by the Ministry of Education (2014R1A1A2057136).

## References

1. T. P. Moffat and D. Josell, *J. Electrochem. Soc.*, **159**, D208 (2012).
2. D. Josell and T. P. Moffat, *J. Electrochem. Soc.*, **161**, D287 (2014).
3. K. H. Kim, T. Lim, M. J. Kim, S. Choe, K. J. Park, S. H. Ahn, O. J. Kwon, and J. J. Kim, *J. Electrochem. Soc.*, **161**, D756 (2014).
4. S. K. Cho, M. J. Kim, H.-C. Koo, O. J. Kwon, and J. J. Kim, *Thin Solid Film*, **520**, 2136 (2012).
5. J.-J. Yan, L.-C. Chang, C.-W. Lu, and W.-P. Dow, *Electrochim. Acta*, **109**, 1, (2013).
6. Y.-T. Lin, M.-L. Wang, C.-F. Hsu, W.-P. Dow, S.-M. Lin, and J.-J. Yang, *J. Electrochem. Soc.*, **160**, D3149 (2013).
7. T. Hayashi, S. Matsuura, K. Kondo, K. Kataoka, K. Nishimura, M. Yokoi, T. Saito, and N. Okamoto, *J. Electrochem. Soc.*, **162**, D203 (2015).
8. K. Kondo, C. Funahashi, Y. Miyake, Y. Takeno, T. Hayashi, M. Yokoi, N. Okamoto, and T. Saito, *J. Electrochem. Soc.*, **161**, D791 (2014).
9. H. C. Kim, S. Choe, J. Y. Cho, D. L. I. Jung, W.-S. Cho, M. J. Kim, and J. J. Kim, *J. Electrochem. Soc.*, **162**, D109 (2015).
10. M. J. Kim, Y. Seo, H. C. Kim, Y. Lee, S. Choe, Y. G. Kim, S. K. Cho, and J. J. Kim, *Electrochim. Acta.*, **163**, 174 (2015).
11. S.-K. Kim, D. Josell, and T. P. Moffat, *J. Electrochem. Soc.*, **153**, C616 (2006).
12. S.-K. Kim, S. Hwang, S. K. Cho, and J. J. Kim, *Electrochem. Solid-State Lett.*, **9**, C25 (2006).
13. A. Chrzanowska, R. Mroczka, and M. Florek, *Electrochim. Acta.*, **106**, 49 (2013).
14. L. Oniciu and L. Muresan, *J. Appl. Electrochem.*, **21**, 565 (1991).
15. H. C. Kim, M. J. Kim, S. Choe, T. Lim, K. J. Park, K. H. Kim, S. H. Ahn, S.-K. Kim, and J. J. Kim, *J. Electrochem. Soc.*, **161**, D749 (2014).
16. I. Volov, X. Sun, G. Gadikota, P. Shi, and A. C. West, *Electrochim. Acta*, **89**, 792 (2013).
17. T. P. Moffat, D. Wheeler, and D. Josell, *J. Electrochem. Soc.*, **151**, C262 (2004).
18. T. P. Moffat, D. Wheeler, S.-K. Kim, and D. Josell, *J. Electrochem. Soc.*, **153**, C127 (2006).
19. P. Broekmann, A. Fluegel, C. Emnet, M. Arnold, C. Roeger-Goepfert, A. Wagner, N. T. M. Hai, and D. Mayer, *Electrochim. Acta*, **56**, 4724 (2011).
20. N. T. M. Hai, K. W. Krämera, A. Fluegel, M. Arnold, D. Mayer, and P. Broekmann, *Electrochim. Acta*, **83**, 367 (2012).
21. N. T. M. Hai, T. T. M. Huynh, A. Fluegel, M. Arnold, D. Mayer, W. Reckien, T. Bredow, and P. Broekmann, *Electrochim. Acta*, **70**, 286 (2012).
22. S.-K. Kim and J. J. Kim, *Electrochem. Solid-State Lett.*, **7**, C98 (2004).
23. J. J. Kim, S.-K. Kim, and Y. S. Kim, *J. Electroanal. Chem.*, **542**, 61 (2003).
24. E. Garcia-Cardona, E. H. Wong, and D. P. Barkey, *J. Electrochem. Soc.*, **158**, D143 (2011).
25. M. A. Pasquale, A. E. Bolzan, J. A. Guida, R. C. V. Piatti, A. J. Arvia, O. E. Piro, and E. E. Castellano, *Solid State Sci.*, **9**, 862 (2007).

Downloaded on 2019-09-03 to IP 49.247.202.102 address. Redistribution subject to ECS terms of use (see ecsdl.org/site/terms_use) unless CC License in place (see abstract).

26. S. Choe, M. J. Kim, H. C. Kim, S. K. Cho, S. H. Ahn, S.-K. Kim, and J. J. Kim, *J. Electrochem. Soc.*, **160**, D3179 (2013).
27. S. Choe, M. J. Kim, H. C. Kim, T. Lim, K. J. Park, K. H. Kim, S. H. Ahn, A. Lee, S.-K. Kim, and J. J. Kim, *J. Electroanal. Chem.*, **714–715**, 85 (2014).
28. A. Barriola, J. I. Miranda, M. Ostra, and C. Ubide., *Anal. Bioanal. Chem.*, **398**, 1085 (2010).
29. M. Ostra, C. Ubide, and M. Vidal, *Anal. Bioanal. Chem.*, **399**, 1907 (2011).
30. A. Barriola, E. Garcia, M. Ostra, and C. Ubide, *J. Electrochem. Soc.*, **155**, D480 (2008).
31. W.-H. Wang and C.-C. Hung,, S.-C. Chang and Y.-L. Wang, *J. Electrochem. Soc.*, **157**, H131 (2010).
32. C.-C. Hung, W.-H. Lee, S.-Y. Hu, S.-C. Chang, K.-W. Chen, and Y.-L. Wang, *J. Vac. Sci. Technol. B*, **26**, 255 (2008).
33. W. Wang, Y.-B. Li, and Y.-L. Li, *Appl. Surf. Sci.*, **255**, 4389 (2009).
34. L. D'Urzo, H. Wang, A. Pa, and C. Zhi, *J. Electrochem. Soc.*, **152**, C243 (2005).
35. L. D'Urzo, H. Wang, C. Tang, A. Pa, and C. Zhi, *J. Electrochem. Soc.*, **152**, C697 (2005).
36. J. P. Healy and D. Pletcher, *J. Electroanal. Chem.*, **338**, 167 (1992).
37. L. T. Koh, G. Z. You, S. Y. Lim, C. Y. Li, and P. D. Foo, *Microelectron. J.* **32**, 973 (2001).
38. L. T. Koh, G. Z. You, C. Y. Li, and P. D. Foo, *Microelectron. J.* **33**, 229 (2002).
39. G. Chalyt, P. Bratin, M. Pavlov, A. Kogan, and M. J. Perpich, U.S. Pat. 6572753 (2003).
40. Z.-W. Sun, C. Yu, B. Metzger, D. W. Nguyen, and G. Dixit U.S. Pat. 6808611 (2004).
41. C. D. Ellis, M. C. Hamilton, J. R. Nakamura, and B. M. Wilamowski, *IEEE Trans. Compon. Packag. Manuf. Technol.*, **4**, 1380 (2014).
42. B.-G. Xie, J.-J. Sun, X.-B. Chen, J.-H. Chen, T.-L. Xiang, and G.-N. Chen, *J. Electrochem. Soc.*, **154**, D516 (2007).
43. S. Choe, M. J. Kim, K. H. Kim, H. C. Kim, J. C. Song, S.-K. Kim, and J. J. Kim, *J. Electrochem. Soc.*, **162**, H294 (2015).
44. M. Pavlov, E. Shalyt, and P. Bratin, U.S. Pat. 7291253 (2007).
45. T. P. Moffat and L.-Y. O. Yang, *J. Electrochem. Soc.*, **157**, D228 (2010).
46. T. P. Moffat, B. Baker, D. Wheeler, and D. Josell, *Electrochem. Solid-State Lett.*, **6**, C59 (2003).
47. M. Tan, C. Guymon, D. R. Wheeler, and J. N. Harb, *J. Electrochem. Soc.*, **154**, D78 (2007).
48. F. J. Monahan, J. B. German, and J. E. Kinsella, *J. Agric. Food Chem.*, **43**, 46 (1995).


Downloaded on 2019-09-03 to IP **49.247.202.102** address. Redistribution subject to ECS terms of use (see **ecsdl.org/site/terms_use**) unless CC License in place (see abstract).